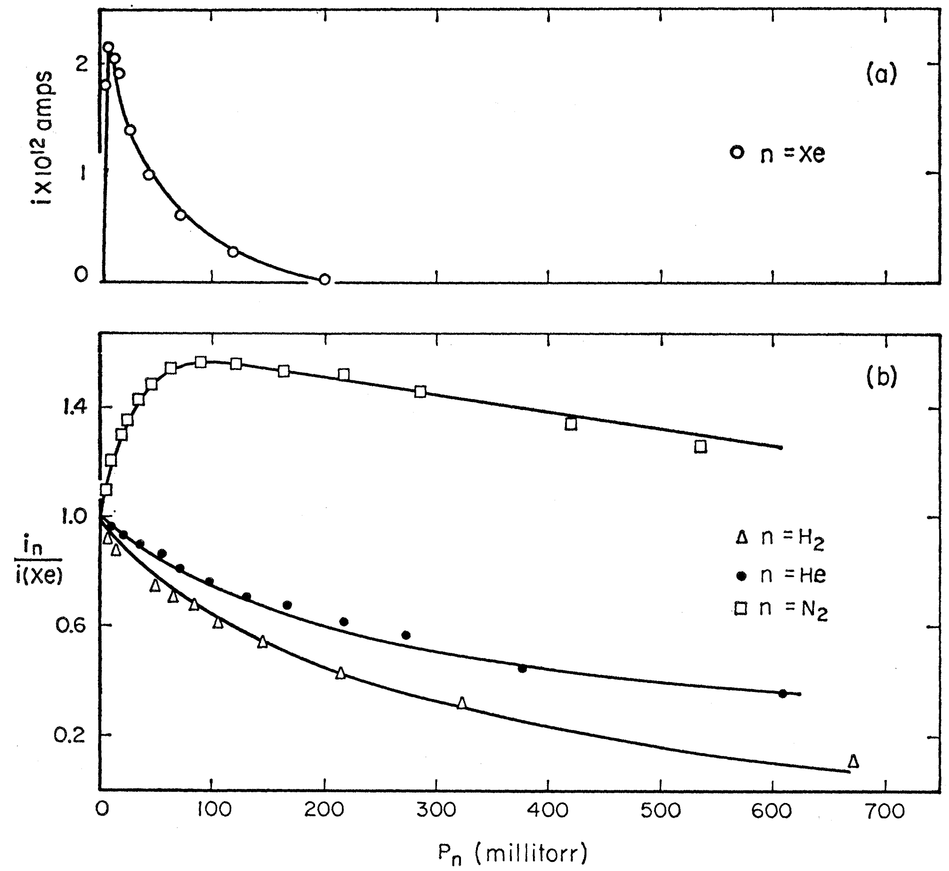

Fig. 1. (*a*) Current flow as a function of xenon pressure. (*b*) Effect of hydrogen, helium, and nitrogen on the ratio i_n/i(Xe).

had no effect on the observed current. Any effects due to the small amount of 1295-Å radiation emitted by the lamp (*1*) are therefore negligibly small. Since the ionization potentials of Xe, H_2, He, and N_2 are all greater than 10 volts, ionization of any of these species in their ground state cannot occur with a 4-volt collection potential and do not contribute to the observed current.

The sharp current increase below 5 mtorr of Xe is due to two processes: (i) the ejection of photoelectrons by 1470-Å radiation imprisoned in the reaction vessel and (ii) the ejection of electrons from the gold electrode by the $6S[3/2]^0_1$ (8.44 ev) and $6S[3/2]^0_2$ (8.31 ev) excited states of xenon. Radiation imprisonment increases the effective lifetime of the $6S[3/2]^0_1$ state so that it can be collisionally deactivated to the metastable $6S[3/2]^0_2$ state as well as eject electrons from the gold surface. Due to the strong resonance absorption (*2*), a greater fraction of the excited atoms is produced closer to the LiF window as the pressure is increased. Consequently deactivation of the excited atoms by collision with the vessel wall near the window becomes increasingly important, so that the rate of electron ejection from the gold surface decreases as the pressure of xenon increases above 5 mtorr.

Figure 1*b* is a plot of the ratio i_n/i(Xe) as a function of pressure of H_2, He, and N_2. The quantity i(Xe) is the current obtained when 5 mtorr of Xe alone is irradiated by the resonance lamp and i_n is the current observed when gas n at pressure P_n is added to the Xe. Both He and H_2 decrease the current signal monotonically as the pressure is increased, whereas the addition of N_2 results in a signal increase, with a broad maximum at about 100 mtorr. No significant current above the background photoelectric effect is observed in the absence of the Xe.

Since H_2, He, and N_2 are all transparent at 1470-Å radiation they have no direct effect on the 1470-Å photons trapped in the reaction vessel. Figure 1*b* shows that H_2 is a more effective quenching agent than He. This is probably due to a contribution by the process (*3*): $Xe^* + H_2 \longrightarrow 2H + Xe$, where Xe* is the activated state of Xe. The repulsive $^3\Sigma$ state of H_2 is 6 to 8 volts above the ground state and is readily excited by collision with either a $6S[3/2]^0_1$ or a $6S[3/2]^0_2$ xenon atom.

The increase of the i_n/i(Xe) ratio upon the addition of nitrogen can only be accounted for by collisional excitation to one or more of the several metastable states (*4*) of N_2 lying below 8.44 ev. These excited N_2 molecules can diffuse to the gold surface and eject electrons The deactivation of these states by other N_2 molecules has been shown to be inefficient (*5*), so that the broad maximum observed in Fig. 1*b* is reasonable.

Thus xenon atoms excited by 1470-Å radiation are quenched more efficiently by H_2 than by He. Nitrogen, on the other hand, is capable of collisional excitation to one or more of several possible metastable states which are detected by their ability to eject electrons from a gold surface.

WILLIAM M. JACKSON*
MILTON D. SCHEER
National Bureau of Standards,
Washington, D.C.

References

1. H. Okabe, *J. Opt. Soc. Am.* **54**, 478 (1964).
2. J. R. Dacey and J. W. Hodgins, *Can. J. Res. Section B* **28**, 90 (1950).
3. H. R. Calvert, *Z. Physik* **78**, 479 (1932).
4. G. Herzberg, *Molecular Spectra and Molecular Structure I* (Van Nostrand, Montreal, 1950).
5. J. F. Noxon, *J. Chem. Phys.* **36**, 926 (1962).
6. One of us (W.M.J.) is a NRC-NSF postdoctoral associate.

* Present address: Goddard Space Flight Center, NASA, Greenbelt, Maryland.

7 January 1965

■

Fossil Bacteria in Pyrite

Abstract. *A considerable variety of bacteria and similar microorganisms are present as preserved remains in pyrite samples of Pennsylvanian age obtained from the coal measures of southeastern Ohio. The types observed are similar to the present-day microflora found in stagnant pools of low oxygen and nutrient content.*

Various pyrite-containing samples from the Pennsylvanian and Mississippian coal formations of southeastern Ohio were collected as part of a study of the origin of acid mine drainage. Fossil bacteria were accidentally discovered in samples from Middle Kittanning (No. 6) Coal from northeastern Vinton County, Ohio. Other workers (*1*) have emphasized the improbability of finding identifiable bacterial remains in ancient sediments. It now appears that with electron microscopy much more evidence may be disclosed than was previously thought to exist.

Fig. 1. Line tracing prepared from a replica micrographic mosaic, showing irregular lineation of *Sphaerotilus* cells. Cells filled with pyrite show a thin cell wall outline. The replica from which the micrographs were made split transversely because of the electron bombardment during viewing. The split is shown here by a narrow gap across the middle of the drawing. (× 2500)

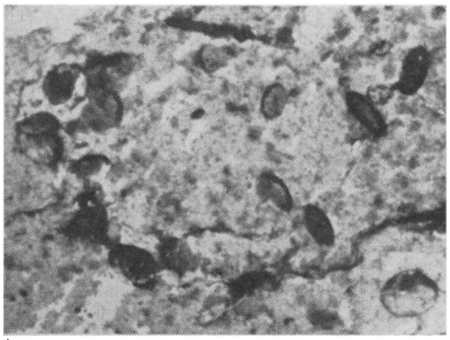

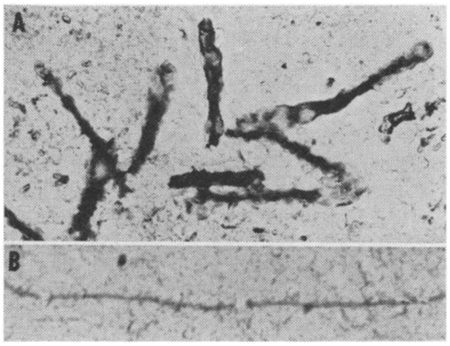

Fig. 2 (left). Replicas of aggregations of ovoidlenticular, unicellular microfossils from pyrite replicas. The heavy cell wall is probably organic; variations in density and thickness of the wall may be due both to differences incidental to preservation and to replication. Except for smaller dimensions and greater numbers of lenticulas, the cells seem to resemble the green unicellular alga *Chlorella pyrenoidosa*. (Shadow-cast with gadolinium; × 7500) Fig. 3 (right). Replicas of rod-shaped bacteria preserved in pyrite. (*A*) The irregularly shrunken bacterial rods which show a smooth marginal halo in some areas suggest an early stage in the formation of the mineral matrix which differs from a subsequent "collapse" stage of mineralization. The darkest cell wall outlines (for example, see the vertically aligned cell in the center) are almost certainly composed of organic matter. (× 7500) (*B*) A chain of completely collapsed rod-shaped bacterial cells of the *Sphaerotilus* type. The dark line of the bacterial cells probably consists of a residue of organic matter. (× 15,000)

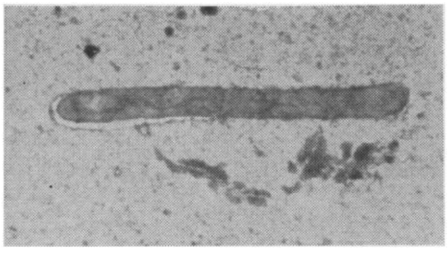

Fig. 4. Rod-shaped bacterium with a suggestion of transverse division and irregular longitudinal striation. These features and the darker image may result from fossil organic matter within the pyrite that has been retained by the replica. According to this interpretation, the film of organic material may have pulled away from its expanded area owing to electron bombardment. Alternatively, the crack caused by shrinkage might represent alteration during mineral deposition. (Shadow-cast with gadolinium; × 7600)

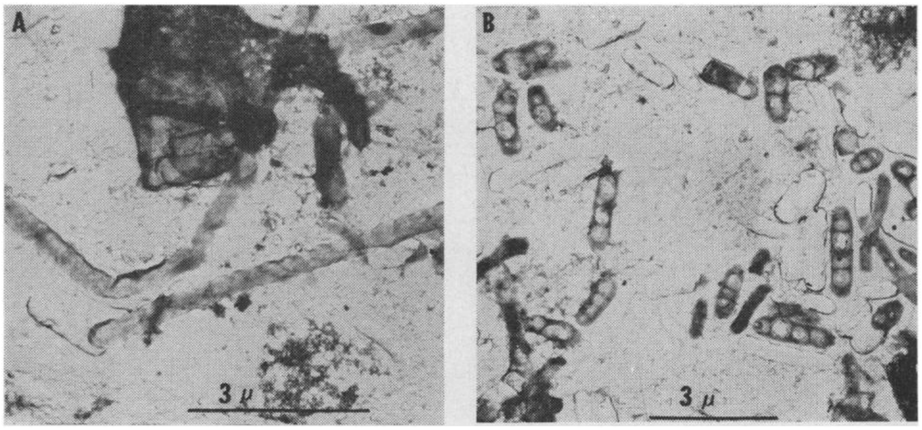

Fig. 5. (*A*) Spiral stalks of *Gallionella*. Darker texture of the stalk replica suggests that some organic matter may have persisted. The dark areas left of center suggest external moulds of unidentified microbial fossils. "Pseudopodia" extending from them may be artifacts of preservation. (*B*) Segmented microbes with cellular contents. Spheroidal granules, one per cell wherever they are present, may represent the residue of an original cytologic feature. Dark cells are those in which organic material has detached from the pyrite and adhered to the replica. Many examples are shown in which only the outline is present in replica and the fossil substance has been retained by the pyrite surface from which the replica was stripped. (Shadow-cast with gadolinium; *A*, × 7850; *B*, × 5350)

The samples were prepared as follows. The pyrite was cut, ground, and given a final polish with 0.25-μ diamond paste on a silk lap. The samples were kept in a humid atmosphere for 3 days at 60°C in order to promote oxidation; they were then washed with acetone. Replicas for electron microscopy were prepared by first allowing several drops of liquid collodion to dry on the surface. This was stripped off with cellophane tape; a thin layer of carbon was precipitated on the collodion surface by the standard arc method in a vacuum. The sample was shadow-cast with gadolinium, and immersed in a solution of amyl acetate and isopropyl alcohol. The tape and collodion were dissolved after several hours, and the carbon-gadolinium replica (which floated to the surface) was netted with a 100-mesh copper grid. Examination of the replicas was made with a Philips EM100 electron microscope.

A considerable variety of bacteria and other microorganisms were observed—among them representatives of iron bacteria which Winogradsky (*2*) considered to be chemoautotropic, such as forms similar to those referred to as *Sphaerotilus* by Pringsheim (*3*), which are shown as line drawings in Fig. 1. Examples of other types, such as *Gallionella*, which probably also represent microflora from stagnant pools of low oxygen and low nutrient content are shown in Figs. 2 to 5.

To establish that the bacteria were truly contemporaneous with the pyrite, and not a recent contamination of the sample, the pyrite sample was immersed in weak nitric acid for several minutes. This treatment is known to etch pyrite, but has no effect on organic matter. Additional replicas of the same areas clearly showed that both the pyrite and bacterial remains are etched to a similar extent. This demonstrates that the bacteria were to a large extent replaced by pyrite. The darker textures of some of the bacterial remains on the replicas in Figs. 2 to 5 indicate that some organic matter persists in the remains.

It seems reasonable to assume, in view of the fact that the bacteria are intimately associated with an iron sulfide nodule, that these microorganisms were probably similar in function to contemporary types which they also resemble in appearance. This assumption has been made for the several cases of fossil bacteria previously observed (*4*, *5*). Contemporary iron-producing bacteria cause $Fe(OH)_3$ to form within the sheath. Hydrogen sulfide, which would be accessible in organic decay processes, could react with the bacterial remains to form pyrite.

One question to be answered is whether this is a freak demonstration, or whether microbiological inclusions may be expected in most coal measures. Probably an abundant microbiological record is preserved in some types of authigenic deposits such as pyrite, but special techniques are needed to disclose it. The resolution required for observation is provided by the electron microscope, but a very delicate etching and replication technique must be used or the evident structure of the fossils will either remain invisible or be destroyed. There is every reason to believe that a wider search for the remains of microorganisms by appropriate similar methods would be successful (*5*).

ERNEST G. EHLERS
DAVID V. STILES
JOHN D. BIRLE
Department of Mineralogy, Ohio State University, Columbus

References and Notes

1. K. L. Temple, *Econ. Geol.* **59**, 1473 (1964).
2. S. Winogradsky, *Botan. Zeitung*, **46**, 262 (1888).
3. E. G. Pringsheim, *Phil. Trans. Roy. Soc. London Ser. B*, **232**, 311 (1946).
4. S. I. Kuznetsov, M. W. Ivanov, N. L. Lyalikova, *Introduction to Geological Microbiology* (McGraw-Hill, New York, 1963), pp. 50–60.
5. J. Schopf, E. G. Ehlers, D. V. Stiles, J. D. Birle, *Proc. Am. Phil. Soc.*, in press.
6. We thank Dr. James Schopf for his extensive assistance in preparing this report and NIH for financial support (grant WP-00340).

1 February 1965

Cryogenic Cooling by Noncondensible-Gas Injection

Abstract. *Temperature control of various cryogenic liquids in the range from their boiling points to near or below their freezing points has been achieved by injecting a noncondensing gas, helium. The process is more easily accomplished than the usual vapor-pumping technique and is applicable in the range from 15° to 300°K. Interesting ice formations were observed in liquid argon.*

Cooling of liquids by evaporation into bubbles of an injected noncondensing gas is a well-known concept that has not been widely applied in laboratory cryogenics. However, Larsen *et al.* (*1*) and Schmidt (*2*) have discussed the theory and presented experimental data on the injection of helium gas into liquid hydrogen or oxygen in a rocket-motor environment.

We present data on the cooling of various liquids by injection of helium gas. Our results indicate that temperature control below the boiling point of the coolant can be achieved more simply by injection of helium than by the usual vapor-pumping technique. The coolants available limit the temperature range of application from 15° to 300°K. The evaporative-cooling effect is strikingly demonstrated by ice formations in liquids having narrow liquid-temperature intervals, such as argon.

The experiments were conducted in a conventional, glass, double-Dewar flask that was strip-silvered to permit visual examination of the inside. The inner flask is shown schematically in Fig. 1; the central container held about 2 liters and was half-filled with coolants for the experiments. The outer flask was filled with a coolant having a boiling point the same as or higher than that of the content of the inner flask in order to make the thermal shielding as neutral as possible. To minimize inflow of ambient heat, the inlet and outlet tubes were constructed of thin-walled stainless-steel tubing or glass. The significance of the (optional) heat exchanger will be noted later. Temperatures were measured with calibrated copper-constantan thermocouples to an accuracy within about 0.1°K. The injection gas was supplied from storage bottles equipped with standard gauges and regulators. Gas flow could be measured accurately within 20 percent. The outlet gas was vented to the atmosphere.

Although any noncondensing gas will produce cooling when bubbled through a liquid, helium is the best for cooling by injection because it has a lower condensation temperature than any other gas, low solubility, low heat-capacity, and good heat-conductive properties; it is also readily available, nontoxic, and nonexplosive. The data reported here were all obtained with helium.

When a noncondensing gas is injected into a liquid, part of the liquid evaporates into the gas bubbles. The change of state of the liquid, from liquid to gas, extracts heat from the liquid; the heat passes into the vapor

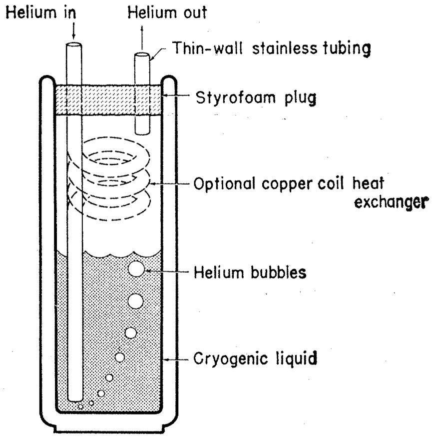

Fig. 1. Schematic drawing of inner flask assembly.

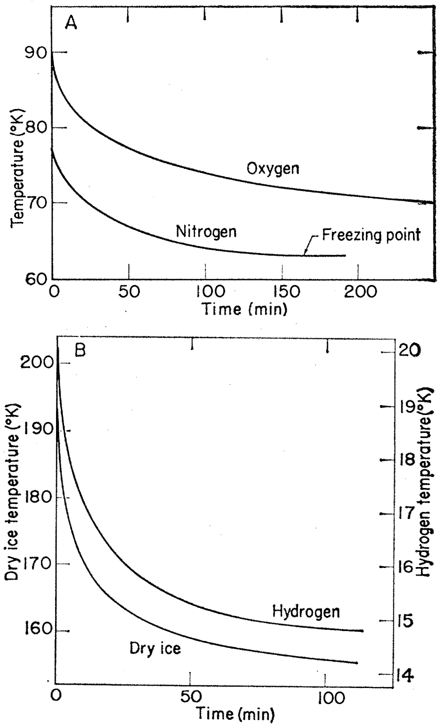

Fig. 2. Temperature versus time for liquid oxygen and liquid nitrogen (*A*) and liquid hydrogen and solid dry ice (*B*) cooled by helium flow at 40 cm^3/sec.